Multiferroicity due to charge ordering

2008 J. Phys.: Condens. Matter 20 434217

(http://iopscience.iop.org/0953-8984/20/43/434217)

IOP PUBLISHING JOURNAL OF PHYSICS: CONDENSED MATTER

J. Phys.: Condens. Matter **20** (2008) 434217 (12pp) doi:10.1088/0953-8984/20/43/434217

REVIEW ARTICLE

Multiferroicity due to charge ordering

Jeroen van den Brink[1,2] **and Daniel I Khomskii**[3]

[1] Institute Lorentz for Theoretical Physics, Leiden University, PO Box 9506, 2300 RA Leiden, The Netherlands
[2] Institute for Molecules and Materials, Radboud Universiteit Nijmegen, PO Box 9010, 6500 GL Nijmegen, The Netherlands
[3] II Physikalisches Institut, Universität zu Köln, 50937 Köln, Germany

E-mail: brink@lorentz.leidenuniv.nl and khomskii@ph2.uni-koeln.de

Received 7 March 2008, in final form 24 April 2008
Published 9 October 2008
Online at stacks.iop.org/JPhysCM/20/434217

Abstract

In this contribution to the special issue on multiferroics we focus on multiferroicity driven by different forms of charge ordering. We will present the generic mechanisms by which charge ordering can induce ferroelectricity in magnetic systems. There is a number of specific classes of materials for which this is relevant. We will discuss in some detail (i) perovskite manganites of the type (PrCa)MnO_3, (ii) the complex and interesting situation in magnetite Fe_3O_4, (iii) strongly ferroelectric frustrated $LuFe_2O_4$ and (iv) an example of a quasi-one-dimensional organic system. All these are 'type-I' multiferroics, in which ferroelectricity and magnetism have different origins and occur at different temperatures. In the second part of this article we discuss 'type-II' multiferroics, in which ferroelectricity is completely *due to* magnetism, but with charge ordering playing an important role, such as (v) the newly discovered multiferroic Ca_3CoMnO_6, (vi) possible ferroelectricity in rare earth perovskite nickelates of the type $RNiO_3$, (vii) multiferroic properties of manganites of the type RMn_2O_5, (viii) perovskite manganites with magnetic E-type ordering and (ix) bilayer manganites.

(Some figures in this article are in colour only in the electronic version)

1. Introduction

Recently there has been a new surge of interest in multiferroics (MFs), single phase compounds in which magnetism and ferroelectricity coexist [1, 2]. Such materials are relatively rare, which raises the fundamental question of what possible mechanisms for multiferroic behavior can exist [3, 4]. Here we consider multiferroicity that is driven by different forms of charge ordering.

1.1. Type-I and type-II multiferroics

Crudely, one can divide multiferroics into two groups[4]. In type-I multiferroics ferroelectricity (FE) and magnetism have different origins and are often due to different active 'subsystems' of a material. In such type-I multiferroics the magnetic order parameter, breaking time reversal symmetry, and the ferroelectric order parameter, breaking spatial inversion symmetry, coexist and have a certain coupling between them.

In the materials that belong to the class of type-I multiferroics the FE can have a number of possible microscopic origins [4]. A cause of ferroelectricity can be (i) the presence of a transition metal (TM) with d^0 configuration, just as in $BaTiO_3$; (ii) the presence of bismuth or lead where the FE is predominantly due to lone pairs of Bi^{3+} and Pb^{2+}; (iii) the presence of 'geometric' ferroelectricity as in $YMnO_3$, where FE is caused by a rotation of rigid M–O polyhedra (in this case MnO_5 trigonal bi-pyramids). In general in these type-I materials the FE ordering temperature is much higher than the magnetic one.

In type-II multiferroics ferroelectricity occurs *only* in the magnetically ordered state: ferroelectricity sets in at the same temperature as a certain type of magnetic ordering and is driven by it. Spiral magnetic ordering, for example, can give rise to type-II multiferroicity [5, 6].

[4] We have in mind homogeneous systems, not the multicomponent ones.

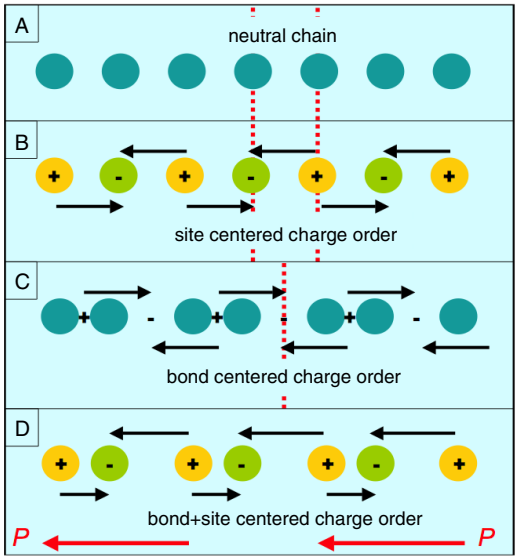

Figure 1. (A) Example of a neutral one-dimensional chain exhibiting (B) site-centered charge ordering, (C) bond-centered charge ordering, and (D) a linear combination of these two that is ferroelectric. The arrows indicate the polarization, which is in total zero in (B) and (C), but develops a macroscopic moment, indicated by the red arrow in (D). The red dashed lines in (A), (B) and (C) indicate mirror planes of the system.

A special group of multiferroics is materials in which ferroelectricity is caused by the charge ordering (CO); these systems are the focus of the present paper. Most of such MFs and potential MFs that we will discuss are of type I: the perovskite manganites (PrCa)MnO_3 [7, 20, 21], magnetite Fe_3O_4 [33–37], quasi-one-dimensional organics [48], and the frustrated charge ordered system $LuFe_2O_4$ [44]. The complex manganites RMn_2O_5 [62] are probably the first example of type-II multiferroics in which FE is due to the simultaneous presence of sites with different charges and with inequivalent bonds occurring in a magnetically ordered state. Another such example is the recently discovered MF in Ca_3CoMnO_6 [51]. We will discuss the observation that the combination of CO and magnetism may also cause MF behavior in rare earth nickelates $RNiO_3$ and point out that related physics explains MF behavior of perovskite manganites with magnetic E-type ordering, as well as of particular bilayer manganites with CO.

1.2. How charge ordering can induce ferroelectricity

The essential mechanism by which charge ordering can lead to the appearance of ferroelectricity is easily explained with the help of the schematic picture shown in figure 1. In figure 1(A) a homogeneous crystal (a one-dimensional chain in this case) with equal (say zero) charge on each site is shown. Figure 1(B) shows the same chain after a charge ordering at which *the sites* become inequivalent: one set of sites has charge $+e$ and the other $-e$, as in NaCl. This process does not breaks spatial inversion symmetry, so that the resulting state cannot have a net dipole moment. This is made explicit in figure 1(B) by marking mirror planes of the charge ordered structure.

Another type of charge ordering occurs when a system dimerizes; see figure 1(C). Such a lattice dimerization can have different origins, e.g. a Peierls distortion. In this case the sites remain equivalent, but *the bonds* are not, as the strong and weak bonds alternate. One can use the terminology of a site-centered charge ordering or site-centered charge density wave (S-CDW) in the case of figure 1(B), and a bond-centered CO or bond-centered charge density wave (B-CDW) in the case of figure 1(C). Also the B-CDW structure is centrosymmetric and thus cannot be ferroelectric.

If one now combines both types of charge ordering in one system, the situation changes drastically. The situation with simultaneous site- and bond-centered CO is schematically shown in figure 1(D). Clearly, inversion symmetry is broken in this case and each 'molecule' (short bond in figure 1(D)) develops a net dipole moment, so that as a result the whole system becomes FE. Thus solids can become ferroelectric if on top of site-centered charge ordering also a bond dimerization occurs [7].

1.3. Magnetic materials in which charge ordering can induce ferroelectricity

We will see below that the simultaneous presence of inequivalent *sites* and *bonds* can have a number of different origins. In some materials bonds are inequivalent just because of the crystallographic structure, and a spontaneous CO that occurs below a certain ordering temperature drives the inequivalence of the sites. Or vice versa, the material can contain ions with different valences, which after a structural dimerization transition induce FE. These two effects may also occur simultaneously, in which case there is one common phase transition.

The appearance of charge ordering is in itself quite ubiquitous in transition metal compounds. It is often observed in systems with ions that formally have a mixed valence. For instance, half-doped manganites like $La_{1/2}Ca_{1/2}MnO_3$ or $Pr_{1/2}Ca_{1/2}MnO_3$ have one extra electron (or hole) per two Mn, showing charge ordering of formally $Mn^{3+}(d^4)$ and $Mn^{4+}(d^3)$. In these manganites CO typically extends over a large part of the doping phase diagram. For example, in $Pr_{1-x}Ca_xMnO_3$, CO exists for $0.3 < x < 0.85$. For $0.3 < x < 0.5$ the ordering is commensurate with the same periodicity as for $x = 0.5$, but for $x > 0.5$ it becomes incommensurate. Magnetic order sets in at temperatures below the CO temperature. The idea of charge ordering developing a ferroelectric component in such doped manganites was first put forward in [7].

Iron-oxides such as magnetite (Fe_3O_4), which exhibits the famous Verwey transition [26, 27], and $LuFe_2O_4$ [44] have a charge ordering due to the formal presence of both $Fe^{2+}(d^6)$ and $Fe^{3+}(d^5)$. In rare earth (R) nickelates of the type $RNiO_3$ the valence of nickel is 3+, but below a certain temperature a charge disproportionation into formally $Ni^{2+}(d^8)$ and $Ni^{4+}(d^6)$ takes place [28, 29].

Traditionally, one has site-centered ordering in mind when considering CO in such TM compounds. On the most basic level one can view this ordering as an alternation of TM ions with different valencies. However, bond-centered CO is also a

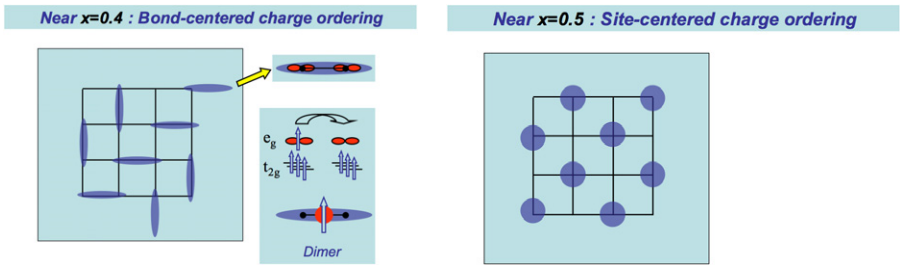

Figure 2. Different types of charge ordering in doped manganites. Left: bond-centered charge ordering of 'Zener polarons' proposed by Daoud-Aloudine *et al* [15]. Right: site-centered CO as proposed in the 1950s [16, 17].

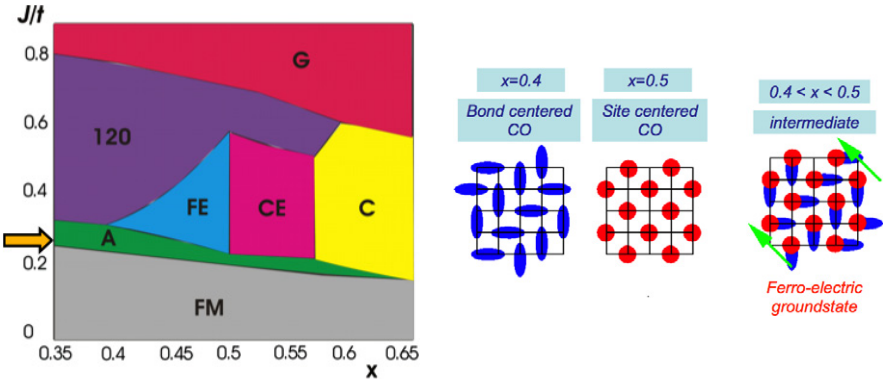

Figure 3. Left: phase diagram of the degenerate double exchange model, by [7]. The arrow indicates a value of the ratio of the effective superexchange J and hopping t for which the sequence of phases as a function of doping is the experimental one. The labels G, 120, A, C, CE, FM and FE denote, respectively, the magnetic G, 120° Jaffet-Kittel, magnetic A, C and CE phases, and ferromagnetic (FM) and ferroelectric (FE) phases. Right: schematic representation of the site- and bond-centered charge ordered states that result in an intermediate ferroelectric state if both types of charge ordering are present simultaneously. The resulting polarization is shown by green arrows.

real possibility. For instance, in many quasi-one-dimensional compounds with partial electron occupation a Peierls transition occurs, which in fact can be viewed as a bond-centered CO, or B-CDW [30]. Generally speaking, this possibility can be also realized in three-dimensional TM compounds like manganites or magnetite. There are however no general rules that tell us whether and when this situation occurs. Each time this question has to be studied separately on a microscopic level.

2. Type-I multiferroics with ferroelectricity due to charge ordering

2.1. Perovskite manganites of the type $Pr_{1-x}Ca_xMnO_3$

The question of whether one or the other (i.e. site- or bond-centered) charge ordering structure (see figure 2) is realized in (PrCa)MnO_3 and whether a ferroelectric state can result from it is experimentally rather controversial. We will review this discussion after presenting the theoretical arguments and calculations that point in the direction of a possible multiferroic ground state in these manganites.

2.1.1. Theoretical situation. In [7, 8] the question of site CO versus bond CO was treated theoretically within a double exchange model that takes into account the double degeneracy of active e_g electrons, as well as the underlying magnetic structure. This approach had proved to be quite successful for overdoped and half-doped manganites before [9–11], and could later even be extended to undoped $LaMnO_3$ [12], which are usually considered as Mott insulators. The results of the computations in the framework of the degenerate double exchange model are presented in the phase diagram of figure 3. The most important result here is the blue 'triangle' to the left of $x \sim 0.5$: in the simplest approximation in this part of the phase diagram the bond-centered CO is lower in energy than the usual site-centered one. The observation that these different charge ordered states are in general very close in energy is confirmed independently by density functional calculations [13, 73].

A more detailed analysis shows that the situation here is actually more complicated and much more interesting: in this region there occurs a *coexistence of site- and bond-centered* CO. In this 'triangular' part of the phase diagram the character of the CO actually changes in a regular way: it evolves from a pure site-centered ground state with magnetic CE-type order at $x = 0.5$, to an admixture of bond-centered state increasing with decreasing x, and finally to a pure bond-centered one at the left edge of the 'triangle' in figure 3. According to our general picture, such a mixed state is FE; see the right panel of figure 3.

One more point is worth mentioning. The theoretical treatment was done for ground states with long-range magnetic ordering. Experimentally, CO in $Pr_{0.6}Ca_{0.4}MnO_3$ sets in at ∼235 K, whereas the Neél temperature is significantly

lower, $T_N \sim 160$ K. However, a recent study indicates that magnetic correlations survive in this system much above the temperature of a long-range three-dimensional magnetic ordering—actually up to T_{CO} [14]. Such short-range magnetic correlations are sufficient for our theoretical approach to be valid.

2.1.2. Experimental situation. For manganites the possibility of a bond-centered charge ordering was first proposed in [15], under the name of a 'Zener polaron' state. On the basis of a detailed structural study of single crystalline $Pr_{1-x}Ca_xMnO_3$ (with $x \sim 0.4$), it was proposed that, contrary to the accepted charge ordering picture [16, 17], shown in the center of the right panel of figure 2, the low-temperature phase of this system is better described not as a site-centered, but as a bond-centered CO. In this bond-centered CO state one extra electron is shared by the pair of neighboring Mn ions, moving back and forth between them, and thus by the double exchange mechanism, orienting the localized spins of their t_{2g} electrons parallel. Hence the terminology 'Zener polaron'—a two-site polaron with ferromagnetic coupling. The proposed bond-centered CO structure of [15] is schematically illustrated in the left panel of figure 2.

The question of whether 'Zener polarons' are present in these doped manganites is hotly debated in the literature. Whereas on the basis of a detailed single-crystal structural study the authors of [15] claim that the bond-centered structure is realized at least for $x = 0.4$, resonant elastic x-ray scattering experiments show that for $x \sim 0.4$–0.5 Mn ions are inequivalent, which was interpreted by Grenier and co-workers as a disproof of the Zener polaron picture [18]. A recent high-resolution transmission electron microscopy and electron-diffraction study, on the other hand, confirms the presence of a 'Zener polaron' state in $Pr_{1-x}Ca_xMnO_3$ [19].

From the theoretical considerations presented above it seems that this controversy is to an extent artificial, as it is based on an oversimplified treatment of the bond-centered CE structure. First of all, theoretical results show that at $x = 0.5$ the conventional site-centered structure with inequivalent Mn ions is indeed realized. But even for $x = 0.4$, where, according to our results [7], Mn–Mn bonds become inequivalent, simultaneously there exists also a site-centered CO, i.e. also the Mn ions should be inequivalent. Thus, the theoretical results reconcile the pictures of [15] and [18] and show that the actual situation is in between, as it combines features of both bond-centered (Zener polaron) and site-centered (checkerboard type) CO. The fact that the actual symmetry of $Pr_{0.6}Ca_{0.4}MnO_3$ is non-centrosymmetric $P11m$ [15] agrees with this picture and, most importantly, with the conclusions that this system should be multiferroic.

A direct observation of ferroelectricity in $Pr_{1-x}Ca_xMnO_3$ could settle the case. Unfortunately, the build-up of a macroscopic polarization is hindered by the finite conductivity of this system, also precluding direct measurement of the polarization. There are at the moment two experimental studies in which an anomaly (a peak) in the dielectric constant ϵ was observed at the CO transition temperature [20, 21], strongly suggesting the presence of ferroelectricity. Two other recent experiments were also interpreted as confirming the presence of FE in $Pr_{1-x}Ca_xMnO_3$ [22, 23].

The anomaly of the dielectric constant at the CO transition was also found in a related system $Pr_{1-x}Na_xMnO_3$ for $x = 0.21$, which corresponds to a hole doping $n_h = 0.42$ [24]. The authors argue that it is a bulk effect, and interpret it as a possible indication of ferroelectricity in this system.

2.2. Fe_3O_4: multiferroic magnetite

The manganites that we discussed in the previous section are not the only, and possibly even not the best, example of ferroelectric and multiferroic behavior that is caused by charge ordering. Another intriguing and famous case is magnetite, Fe_3O_4—the first magnetic material known to mankind (see e.g. [25]), with a ferrimagnetic ordering occurring already below ~860 K. It is also famous because of what apparently is the first example of an insulator–metal transition in TM oxides—the Verwey transition at $T_V = 120$ K [26, 27], a transition that in spite of almost 70 years of dedicated research is still not completely understood. It is much less known, however, that Fe_3O_4 is *ferroelectric* in the insulating state below the Verwey temperature T_V [33–37]. So in addition to all its acclaimed fame, magnetite is probably also one of the first multiferroics.

2.2.1. Charge ordering in magnetite. Fe_3O_4 crystallizes in an inverse cubic spinel structure with two distinct iron positions. The iron B sites are inside an oxygen octahedron and contain two-thirds of the Fe ions, with equal numbers of Fe^{3+} and Fe^{2+}. These sites by themselves form a pyrochlore lattice, consisting of a network of corner-sharing tetrahedra; see figure 4. The iron A sites contain the other one-third of the Fe ions and are not considered relevant for the charge ordering physics. The Verwey metal–insulator transition at $T_V = 120$ K is apparently related to charge ordering transition of the two types of charges that live on the sites of the pyrochlore lattice of the iron B sites. The originally proposed charge ordering pattern [27] consists of an alternation of Fe^{2+} and Fe^{3+} ions in the xy planes at the B sites and was later shown to be too simple. Numerous much more complicated CO patterns were proposed; see e.g. [31] and references therein. The detailed charge ordering pattern is still unresolved.

The difficulty in determining the charge ordering structure is related to the strong frustration of simple bipartite ordering on a pyrochlore lattice, first discussed by Anderson [32]. This frustration has the consequence that there is a macroscopic number of charge configurations with the same ground-state energy, if only nearest-neighbor Coulomb interactions are taken into account. This huge degeneracy remains even in the presence of additional constraints on the possible charge ordering patterns; the best known of these is the so-called Anderson constraint, where each tetrahedron is required to have two Fe^{2+} and two Fe^{3+} ions. Such a macroscopic degeneracy is expected to contribute significantly to the entropy of the system. It was noticed very early on that this situation is very similar to the frustrated order in (water) ice, in which the hydrogen atoms in ice are arranged and constrained

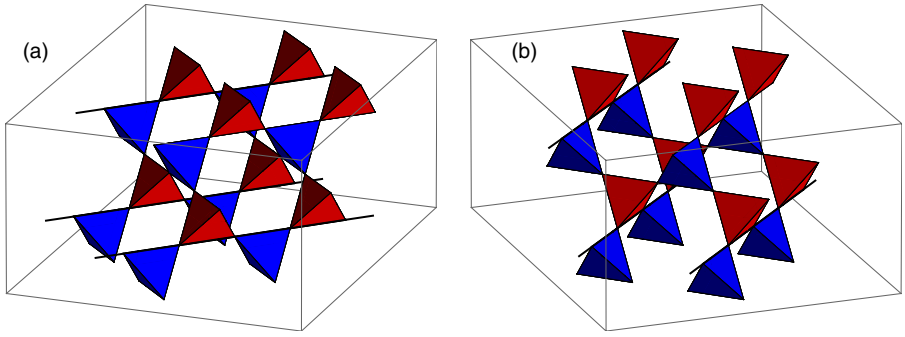

Figure 4. Pyrochlore lattice made by the B sites of a spinel structure from two different viewpoints. In Fe_3O_4 equal numbers of formally Fe^{3+} and Fe^{2+} ions occupy these sites.

according to the so-called Bernal–Fowler rules [38, 39]. Also in the problem of spin-ice frustration is a dominant factor, and its consequences have recently attracted much attention; see for instance [40].

It is clear that residual interactions, beyond the nearest-neighbor Coulomb repulsion, have to be present. These are important and relevant because below T_V magnetite is ordered into a unique ground state. Moreover, a recent high-resolution neutron and x-ray diffraction study by Wright and co-workers [41] concludes that the Anderson rule is violated in Fe_3O_4. But our main point here is that even in the very careful structural investigation of Wright and co-workers a centrosymmetric monoclinic group is used to analyze the diffraction data, which precludes the possibility of a ferroelectric ground state. Thus the real structure of Fe_3O_4 is apparently even more complicated than the ones discussed so far.

2.2.2. Possible origin of ferroelectricity in magnetite. According to [36], the electric polarization P of Fe_3O_4 below the Verwey transition lies in the b-direction. The polarization can be switched by electric field and it leads to the formation of a ferroelectric domain structure that can only be explained by assuming a triclinic crystal structure [42].

The microscopic origin of ferroelectricity in magnetite remains to be unveiled, but one can argue [4, 43] that most probably it is related to the coexistence of site-centered and bond-centered CO of a type that was discussed for the manganites above. Actually, a detailed analysis of the structural data of [41] shows that the situation in this system may be not so far from the one illustrated in the right panel of figure 3. Indeed, in the proposed structural and charge pattern one notices that, besides the site-centered CO—the alternation of the formal Fe^{2+} and Fe^{3+} valence states—there is also a strong modulation of the Fe–Fe distances (the bond lengths). In this structure, shown in figure 5, one sees that e.g. along the Fe chains running in the [110] direction (in the cubic setting), i.e. in the xy chains, there is an alternation of Fe^{2+} and Fe^{3+} ions (open and filled circles in figure 5), but simultaneously there is an alternation of short and long Fe–Fe bonds. This direction corresponds to the monoclinic b-direction, in which the polarization is observed. In this framework each such

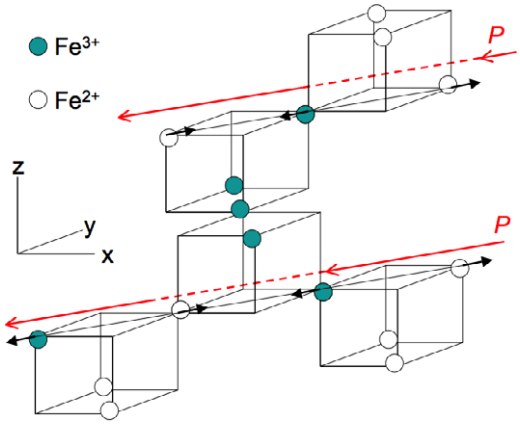

Figure 5. Illustration of the possible origin of ferroelectricity in magnetite. Emphasized are the Fe chains running in the [110] direction of magnetite—a pyrochlore lattice made by the spinel B sites. In the xy chains there is an alternation of Fe^{2+} and Fe^{3+} ions (open and filled circles). Simultaneously, there is an alternation of short and long Fe–Fe bonds; shifts of Fe ions are shown by short black arrows. The resulting polarization is indicated by the long diagonal red arrows.

[110] mixed bond- and site-centered CO chain gives a non-zero contribution to the electrical polarization; cf figure 3.

In the analysis of the structural data in [41] the enforced centrosymmetry is accommodated by a certain pattern of [110] mixed chains that changes into the opposite pattern in the 'upper part' of the unit cell that is doubled in the c-direction. In the enforced centrosymmetric structure Fe_3O_4 is therefore antiferroelectric. How to change the pattern of [41] to incorporate ferroelectricity is not entirely clear at present, but it seems that the main structural features point very strongly in the direction of the mechanism proposed in [7]—the coexistence of bond-centered and charge-centered charge ordering—as the mechanism for ferroelectricity in magnetite.

2.3. Frustrated and charge ordered $LuFe_2O_4$

Recently multiferroicity was observed in $LuFe_2O_4$ [44, 45]. Despite the similarity of its chemical formula to that of a spinel, the structure of $LuFe_2O_4$ is very different from a spinel. It has a double layer structure, with a triangular iron lattice within each layer. The average valence of Fe in it is $Fe^{2.5+}$, similar to

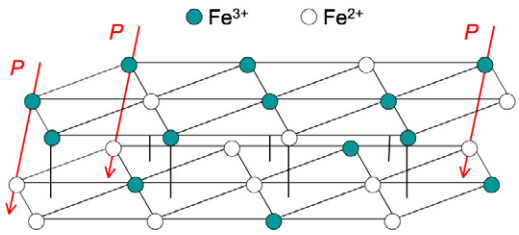

Figure 6. Bilayer of the FeO_2 triangular lattices in $LuFe_2O_4$ with a schematic view of charge redistribution between the layers and the interlayer charge ordering that results in a macroscopic electric polarization indicated by the red arrows.

the B sites in Fe_3O_4, that also nominally have an equal number of Fe^{2+} and Fe^{3+} ions, or one extra electron (or hole) per two sites. Accordingly, charge ordering may occur in $LuFe_2O_4$ and indeed does occur at $T_c = 330$ K.

However, because of the frustrated nature of the triangular iron lattice in each FeO_2 layer, the usual bipartite checkerboard Fe^{2+}/Fe^{3+} charge ordering is not favorable, and another option becomes preferred. A charge redistribution between layers takes place, so that in each bilayer one layer, say the lower layer, has a 2:1 ratio of Fe^{2+}/Fe^{3+} and its upper counterpart has the inverse 1:2 ratio. Because of this interlayer charge redistribution each triangular layer can have a perfect, unfrustrated charge ordering with three sublattices in each triangular layer, one sublattice being occupied e.g. by Fe^{3+}, and two others (forming a honeycomb lattice with these Fe^{3+} at the center of each hexagon) by Fe^{2+}. The charge ordering is vice versa in the other layer; see figure 6. As a result, each *bilayer* acquires a dipole moment, shown in figure 6, and the total system becomes ferroelectric [44–46]. As ferrimagnetic ordering sets in at $T_c = 250$ K, $LuFe_2O_4$ is multiferroic below this temperature.

Thus the FE in $LuFe_2O_4$ is due to a combination of two factors: the bilayer character of the crystal structure, and the frustrated charge ordering leading to the formation of charged planes (e.g. negative charging of the lower layer and positive charging of the upper one). As, generally speaking, in such a situation CO may be very strong, one could in principle expect large spontaneous polarizations—much larger than for example in type-II multiferroics with magnetically driven ferroelectricity [2]. And indeed, the value of the polarization in $LuFe_2O_4$ is 0.24 C m^{-2} [45]—comparable to the polarization of 0.26 C m^{-2} in $BaTiO_3$ [47].

2.4. Quasi-one-dimensional organic materials

A situation that is similar to the one discussed in the previous section—bonds inequivalent just because of the underlying crystal structure, and ferroelectricity caused by charge ordering—exists even in other materials. Probably one of the first such examples is the quasi-one-dimensional organic system $(TMTTF)_2X$ [48]. In this material there is one electron (or rather one hole) per two sites (i.e. per two TMTTF molecules), but the molecular chains are dimerized due to a particular ordering of counter-ions X ($X = PF_6$, AsF_6, SbF_6), which gives rise to inequivalent bonds. With

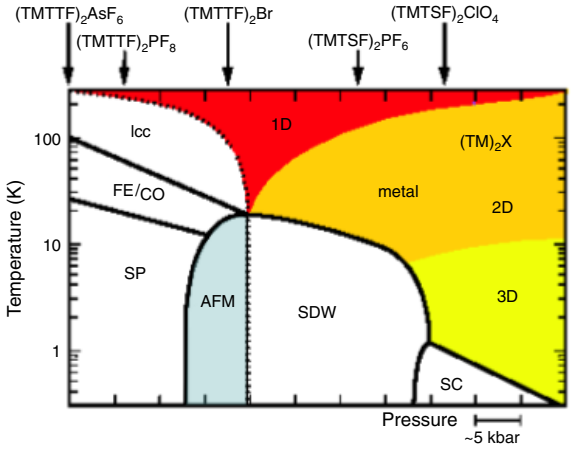

Figure 7. Generic phase diagram of $(TMTTF)_2X$ or $(TMTSF)_2X$ molecular crystals, from [30]. CO—charge-ordered phase; SP—spin–Peierls phase; AFM—the phase with antiferromagnetic ordering; SC—superconducting phase. The charge ordered phase is simultaneously ferroelectric (FE) [48]. In the blue shaded region multiferroicity is expected to occur.

decreasing temperature at $T_{CO} \sim 50$–150 K charge ordering occurs, after which the molecules (sites) become inequivalent, having alternating charge. The situation then becomes exactly the same as the one shown in figure 1(D), and consequently the low-temperature phase of these materials becomes ferroelectric. This is clear from anomalies in the dielectric constant ϵ, which above T_c shows Curie behavior. Below T_{CO} in the simplest picture electrons (or holes) are localized at every second molecule, and the corresponding localized spins either undergo a spin–Peierls transition or have long-range antiferromagnetic ordering when temperature decreases. This behavior is seen in the generic phase diagram of figure 7, adopted from [30]. The spin–Peierls transition would effectively remove magnetism from the picture, but the systems with antiferromagnetic ordering should be classified as multiferroic.

3. Type-II multiferroics with ferroelectricity due to charge ordering and magnetostriction

Magnetically driven FE in type-II multiferroics may have two microscopic origins. One of them, probably the most common, works in systems like $TbMnO_3$ [49], $Ni_3V_2O_8$ [50] and $MnWO_4$ [52–54], in multiferroic pyroxenes [55] and in some other systems. The mechanism of FE in them is usually an inverse Dzyaloshinskii–Moriya effect [57], which operates in systems with non-collinear, usually spiral magnetic structures of a certain type [5, 2]. It requires the direct action of the relativistic spin–orbit interaction.

A second possible mechanism works also for collinear magnetic structures and does not require the presence of spin–orbit coupling: it is based on magnetostriction. For the magnetostriction to give multiferroic behavior one usually requires the presence of inequivalent magnetic ions, with different charges. These, in turn, may be either just different TM ions, or the same element in different valence states. This

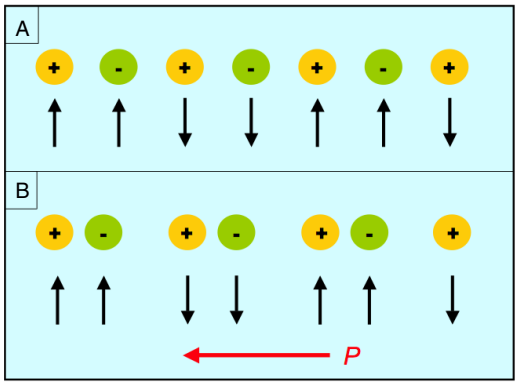

Figure 8. (A) Chain with alternating charges and with the spin structure up–up–down–down. (B) Effect of magnetostriction, shortening (in this example) the ferromagnetic bonds, producing a ferroelectric polarization, indicated by the red arrow in figure 1(D).

mechanism for multiferroicity is illustrated by figure 8. The situation here is almost identical with that shown in figure 1(B). Without spin ordering, the crystal structure is centrosymmetric. The magnetic structure itself is also inversion symmetric, but with a different inversion center. Taking both charge and magnetic structures together, however, the system loses inversion symmetry, i.e. it can become FE. The mechanism of creation of polarization would be the magnetostriction (MS). The MS is definitely different for ferro and antiferro bonds. If energy is gained by shortening of, for example, a ferromagnetic bond, the system will distort as shown in figure 8(B), and one ends up with exactly the same situation as shown in figure 1(D), with unequal bonds and different charges at opposite ends of short 'molecules'. A simple model that exhibits this behavior is the Ising model with both nearest-neighbor and next-nearest-neighbor interactions:

$$H = J_1 \sum_i S_i^z S_{i+1}^z + J_2 \sum_i S_i^z S_{i+2}^z. \qquad (1)$$

If the interaction J_2 is antiferromagnetic (>0) and sufficiently large, $J_2 > 1/2|J_1|$, the magnetic ordering will be of the up–up–down–down type; see figure 8. Depending on the sign of J_1, the bond with parallel spins (for $J_1 < 0$) or with antiparallel ones (for $J_1 > 0$) will shorten, increasing the magnetic energy gain on the corresponding bond. In both cases this will lead to a multiferroic state. An almost ideal realization of this scenario seems to have been found recently in Ca_3CoMnO_6 [51]. In this system with a quasi-one-dimensional structure the ions Co^{2+} and Mn^{4+} alternate along the chain, and magnetic structure is of the up–up–down–down type. Indeed, below $T_N = 16$ K, Choi *et al* observe an electric polarization in this system [51].

3.1. Manganites of the type RMn_2O_5

The manganites RMn_2O_5, where R is a rare earth ion [62], are one of the first examples of type-II multiferroics that were discovered. In these manganites ferroelectricity is presumably driven by magnetostriction. It can occur because the material contains Mn sites that are inequivalent by virtue of the crystallographic structure of the material, with on top of

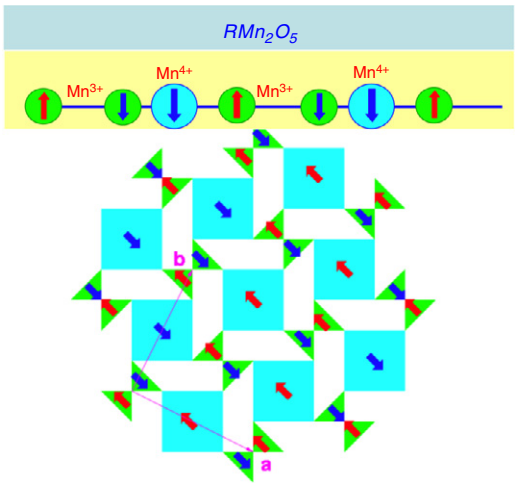

Figure 9. Schematic view of the crystal structure of RMn_2O_5 consisting of connected $Mn^{4+}O_6$ octahedra (blue squares) and $Mn^{3+}O_5$ pyramids (green triangles); the figure is from the review of Sushkov *et al* in this issue. The chain of Mn^{3+}–Mn^{3+}–Mn^{4+} along the b-direction, with corresponding spin ordering, is shown in the upper panel.

this a magnetically driven spontaneous distortion that makes bonds unequal and breaks inversion symmetry. RMn_2O_5 has a rather complicated crystal structure containing inequivalent Mn^{3+} and Mn^{4+} ions in different lattice positions with different oxygen coordinations, with a magnetic ordering that breaks the inversion symmetry of the undistorted, non-ferroelectric lattice [63, 64].

Neutron and x-ray diffraction studies show that these manganites have space group *Pbam* but it is expected that in their multiferroic state the actual symmetry group is $Pb2_1m$, which allows for a macroscopic electric polarization along the b axis [65–67]. The orthorhombic *Pbam* crystal structure of $HoMn_2O_5$ consists of connected $Mn^{4+}O_6$ octahedra and $Mn^{3+}O_5$ pyramids (see figure 9). The octahedra share edges and form ribbons parallel to the c axis. Adjacent ribbons are linked by pairs of corner-sharing pyramids. Below 38 K e.g. in $HoMn_2O_5$ a commensurate magnetic structure develops with propagation vector $\mathbf{k} = (\frac{1}{2}, 0, \frac{1}{4})$, and simultaneously the system becomes ferroelectric [68].

Along the b-direction $HoMn_2O_5$ exhibits a charge and spin ordering that can schematically be denoted as a chain of $Mn^{3+}_{\Uparrow}$–$Mn^{4+}_{\Uparrow}$–$Mn^{3+}_{\Downarrow}$ or ⇓–⇓–⇑, as in figure 9. In the undistorted *Pbam* structure the distances $d_{\Uparrow\Uparrow}$ (between $Mn^{3+}_{\Uparrow}$ and $Mn^{4+}_{\Uparrow}$) and $d_{\Uparrow\Downarrow}$ (between $Mn^{3+}_{\Uparrow}$ and $Mn^{4+}_{\Downarrow}$) are the same. *Ab initio* calculations of the relaxed structure [70–72] reveal a shortening of distances between parallel spins $Mn^{3+}_{\Uparrow}$ and $Mn^{4+}_{\Uparrow}$ ions—in the ferroelectric $Pb2_1m$ structure $d_{\Uparrow\Uparrow} < d_{\Downarrow\Uparrow}$, which optimizes the double exchange energy [2, 7, 63].

3.2. Origin of ferroelectricity in RMn_2O_5

There is still some controversy about the microscopic mechanism of ferroelectricity in this system [2]. The most plausible explanation is the one indicated above: magnetically induced changes in bond lengths between Mn ions with

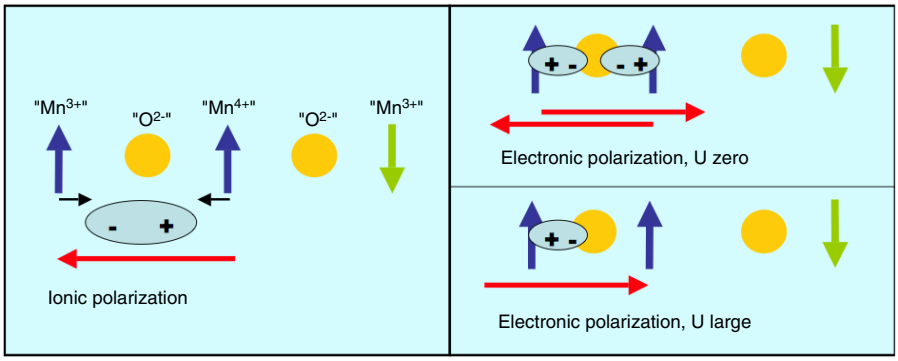

Figure 10. Schematic view of the two contributions to the ferroelectric polarization in RMn_2O_5 in the uncorrelated ($U = 0$) and strongly correlated limit (large U). In the latter the electronic polarization nearly cancels the ionic polarization. The labels '$Mn^{4+/3+}$' indicate Mn ions that have a valence of more/less than 3.5+, respectively.

different formal valences, adding up to a net ferroelectric moment. The actual picture that arises from microscopic electronic structure calculations supports this scenario [70–72], but is actually even more interesting; see below. An alternative picture is that the ferroelectricity in RMn_2O_5 is due to a spiral magnetic structure, as in many other type-II multiferroics [69]; but most probably the weak spiral observed in [69] is not the source, but rather the consequence of ferroelectricity, similar to the case of $BiFeO_3$.

The electronic structure calculations show that the magnetic ordering gives rise to a large *electronic* polarization, inducing a transfer of charge from the Mn sites to the Mn–O–Mn bonds, similar in spirit to the perovskite manganites that we discussed in a previous section. This charge transfer drives the bond-length shortening and gives rise to an ionic polarization as the two Mn ions involved have formally different charges. The transferred charge itself, however, does not induce a large dipole moment, because the charges accumulated on the bonds comes from opposite directions in roughly the same amount [70–72]. However, this changes drastically when the on-site Coulomb interactions between the Mn 3d electrons are accounted for [72]. It depletes electrons from the Mn^{4+} site, making it almost closed shell t_{2g}, and as a consequence its polarization cloud disappears. The overall result is that in these strongly correlated multiferroic manganites a substantial *electronic* polarization develops, which is almost as large as the *ionic* polarization, but opposite in direction; see figure 10. In the end a small net polarization of $P = 82$ nC cm^{-2} results, in very good agreement with the experimental value [72].

3.3. Nickelates of the type $RNiO_3$

In the examples of type-II MF with the magnetostriction mechanism considered above, the different charges of magnetic ions were determined simply by the structure of the compound: in the previous section we discussed different TM ions such as Co^{2+} and Mn^{4+} in Ca_3CoMnO_6 or Mn^{3+} and Mn^{4+} in respectively the pyramids and octahedra of RMn_2O_5. However, inequivalent ions can also appear spontaneously, as a site-centered CO, with bonds becoming different due to magnetostriction. Possible examples of this are certain rare earth nickelates $RNiO_3$ (see also [2]).

These systems are known to have a spontaneous charge disproportionation (or CO) below their metal–insulator transition [28, 29]. This feature is especially prominent when the rare earth is small (Y, Lu). The disproportionation leads to the formation of a rock-salt-like charge structure: alternation of, formally, Ni^{2+} and Ni^{4+} in consecutive [111] planes of the cubic perovskite lattice (for simplicity we ignore orthorhombic tilting in this picture, which can however be important in real materials).

It is still controversial which magnetic structure appears in these systems at temperatures below $T_N < T_{CO}$. One possibility is that it is a sequence of the same [111] planes ordered in ↑↑↓↓ fashion [56]. Another proposed structure is more complicated: it has the same superstructure wavevector $Q = (1/4, 0, 1/4)$ (in an orthorhombic unit cell), but it has Ni^{2+} and Ni^{4+} spins alternating in different directions, and possibly with non-collinear spins [28]. The second structure does not lead to FE, at least not in a straightforward fashion. But the first magnetic structure should naturally give a polarization in the same [111] direction: the distances between ferromagnetic ↑↑ and antiferromagnetic ↑↓ planes should not be the same due to different magnetostrictions of ferro and antiferromagnetic bonds, which, for the alternating charges between these [111] layers would immediately give ferroelectricity, as illustrated in figure 11.

Note that this mechanism for FE is different from the one proposed in [57, 58] for manganites with E-type antiferromagnetic ordering (which is rather similar to the first magnetic structure of nickelates discussed above; figure 11). The mechanism presented in [57] does not require inequivalent charges of TM ions. In addition, it would produce a polarization not in the [111] direction, but in the plane perpendicular to it; see the next section.

3.4. Magnetic E-type $RMnO_3$ manganites

In the perovskite manganite family $RMnO_3$ the magnetic E phase was first reported for R = Ho [59]. The E-type magnetic structure of this multiferroic is schematically shown in figure 12. Here we wish to point out that the established picture of multiferroicity in E-type manganites is actually a realization of the same scenario that we have discussed above,

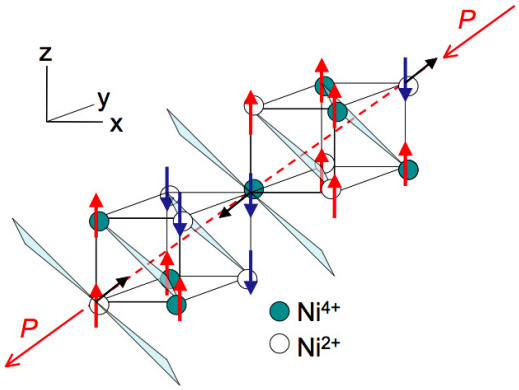

Figure 11. Illustration of simultaneous charge disproportionation in Ni^{2+}/Ni^{4+} (open and filled circles) and magnetic ordering in $RNiO_3$ (red and blue vertical arrows). The real disproportionation will be less ionic and more of the type $Ni^{(3-\delta)+}/Ni^{(3+\delta)+}$. Small black arrows indicate the ionic displacements along the body diagonal of the cubes due to magnetostriction, and the direction of the resulting macroscopic electric polarization P is indicated by the long red diagonal arrow.

of inequivalent bonds and sites combined with striction. Before explaining this in detail, let us retrace our steps for a moment and discuss the E-type materials in a slightly more general context.

As already stated, we can separate type-II multiferroics into to subcategories: those in which ferroelectricity is due to a particular non-collinear (spiral) magnetic structure [5, 2]—with as the microscopic driving mechanism of the polarization an inverse Dzyaloshinskii effect [57], and those in which FE is due to magnetostriction. Examples of the second class are e.g. $RNiO_3$ and RMn_2O_5. These might seem very different systems, but they actually have, as we pointed out, the same physics as discussed in the main part of our paper: inequivalent sites to start with, plus bonds becoming inequivalent due to magnetostriction.

In the materials discussed so far, however, one starts out with TM ions with different charge (different valence). The suggested mechanism of FE in the E-type manganites [60], supported by *ab initio* calculations [58], seems at first glance different: all metal ions have the same valence and charge (Mn^{3+}). However, in fact the situation is rather similar to the one discussed in the previous section, with positively charged Mn^{3+} and negatively charged O^{2-} playing the same role as TM ions with different valences in systems described above. This point is schematically explained in figure 13, which is a simplified representation of the real crystal and magnetic structure of figure 12.

As shown in figures 12, 13, the oxygens are shifted away from their original position at the center of TM–TM bonds, due to the usual tilting of TMO_6 octahedra that is often present in perovskites (the $GdFeO_3$ distortion). Note that at this point all TM–O–TM bonds are still equivalent. However, in the E-type magnetic structure the spin orientation along the TM–O–TM chains is up–up–down–down. To optimize the exchange in FM and AFM bonds the lattice can distort, which in this case, in contrast to figure 1, could be achieved not by longitudinal shifts of the TM ions, but by transverse shifts of the oxygens, modulating the TM–O–TM angles and consequently modifying exchange constants. For localized electrons, according to Goodenough–Kanamori–Anderson rules for superexchange, the strength of a ferromagnetic bond is increased by *decreasing* the TM–O–TM angle (thus moving the oxygens in this bond down in figure 13(A)). To strengthen an AFM bond, however, the TM–O–TM angle should *increase*, approaching 180°. In the

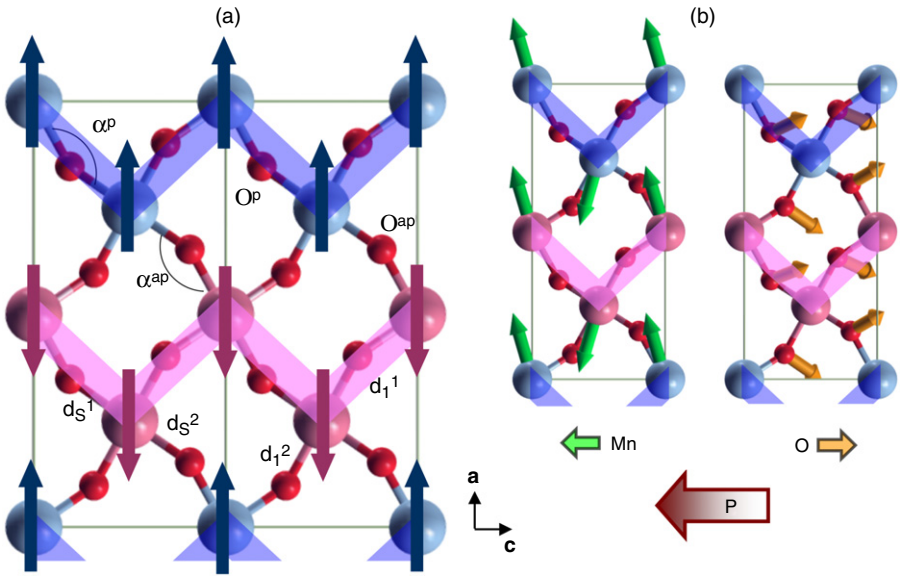

Figure 12. (a) In-plane arrangement of Mn and O atoms in orthorhombic manganites with E-type magnetic structure. Arrows denote the direction of spins and AFM-coupled zigzag spin chains are highlighted by shaded areas. The Mn–O–Mn angle for parallel (α^{p}) and antiparallel (α^{ap}) Mn spins, large (d_l^1 and d_l^2) and small (d_s^1 and d_s^2) Mn–O bond lengths are indicated. (b) Arrows show the directions of the ionic displacements for Mn (left) and O (right) in the AFM E phase. The thick arrows at the bottom show the direction of the resulting displacements of Mn and O sublattices and the polarization P [58].

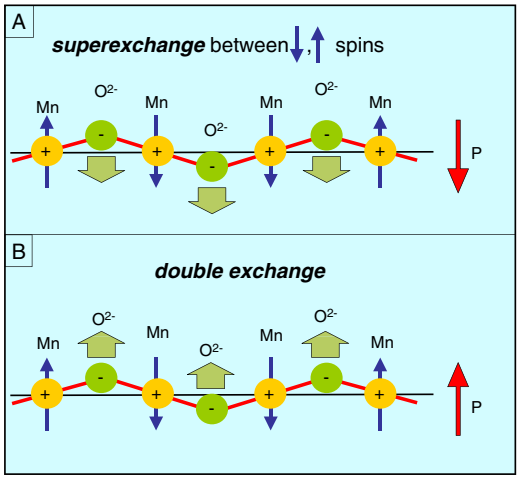

Figure 13. (a) Schematic view of the arrangement of Mn and O atoms in presence of a $GdFeO_3$ distortion. Thin blue vertical arrows denote the direction of Mn spins in the 'straight' Mn chains of the magnetic E-type ordering, cf figure 12. Superexchange drives the Mn–O–Mn angle towards 180° when the spins are antiparallel and away from it when the spins are parallel. Broad green vertical arrows indicate the resulting oxygen displacements; the direction of the ferroelectric polarization is indicated on the right of the chain by the red arrow. (b) Double exchange also causes a ferroelectric polarization, but in the opposite direction. It drives the Mn–O–Mn angle away from 180° when spins are antiparallel and towards it when spins are parallel.

magnetic E phase this requires a shift of respective oxygens in the same direction; see figure 13(A).

It is interesting to note that in the case of double exchange between TM ions the oxygen would shift in the opposite direction: in this situation the ferromagnetic exchange increases with the TM–O–TM angle stretching to 180°, see figure 13(B). This picture applied to the E-type manganites gives the result indicated in the right panel of figure 12(b).

In both cases the net effect is that all negatively charged ions (oxygens) shift in the same direction, which results in a net electrical polarization perpendicular to the chain. One can show that after such a distortion the gain in exchange energy is linear in displacements u, whereas the cost in elastic energy is proportional to u^2, i.e. this process will always be favorable, given the crystal and magnetic structure that we discuss here. Clearly this is a mechanism very similar to the one described earlier in this review. It also relies on the presence of ions with different charges (here positive TM ions and negative oxygens), together with bonds which become inequivalent due to a particular (here E-type) magnetic structure. Such a bond-bending mechanism is apparently rather effective; the corresponding elastic modulus that counteracts such distortion is usually small. Therefore, it can give rise to a rather large polarization [58].

3.5. Bilayer manganite $(LaSr)_3Mn_2O_7$

One more example of multiferroicity that is in its nature related to the charge ordering is observed in the bilayer manganite $(LaSr)_3Mn_2O_7$ [61]. In this paper the evidence for a reorientation of orbital and magnetic stripes below 300 K is presented. After this happened, the situation becomes again similar to that shown in figure 1, with striction plus CO leading to FE. Thus, the mechanism of creation of FE here is similar to the one discussed above, although it remains unclear so far *why* stripes rotate by 90° at this transition.

4. Conclusions

In conclusion, we have described in this paper a generic mechanism that generates ferroelectricity in systems with charge ordering, which, in particular, can lead to multiferroic behavior in transition metal compounds. This mechanism relies on the simultaneous presence of inequivalent sites and bonds. This can occur spontaneously, due to coexistence of site- and bond-centered charge ordering or charge density waves—e.g. in the case of $(PrCa)MnO_3$. The other possibility is that one of these features is a property of the system itself, where either bonds or sites are inequivalent due to the very chemical or crystal structure of the compound. In the case of inequivalent bonds, the sites may become different due to charge ordering; the example of this is organic compounds $(TMTTF)_2X$ or $LuFe_2O_4$. Such systems may be classified as type-I multiferroics—the systems in which magnetism and ferroelectricity have different mechanisms and are in principle independent of each other.

If the sites are different, e.g. have different valences, a bond alternation producing ferroelectricity may occur for example due to magnetostriction. In this case ferroelectricity appears only in a magnetically ordered state with a particular magnetic structure: these systems are type-II multiferroics. However, in contrast to most other multiferroics of this class, this mechanism does not require relativistic spin–orbit coupling—generally a small effect in transition metal compounds.

One of the consequences is that in principle charge ordering-induced multiferroicity may lead to a rather large polarization, comparable to that of a good ferroelectric like $BaTiO_3$ and much larger than in most of the type-II (magnetically driven) multiferroics. The example of $LuFe_2O_4$ demonstrates this. On the other hand, how strong the magnetoelectric coupling in this case will be and what will actually determine it is still an open question. In any case, this mechanism of multiferroic behavior is certainly interesting and promising. Other systems of this type, besides the ones we have discussed in the present paper, will most probably continue to be discovered.

Acknowledgments

We are indebted to a great number of theoretical and experimental colleagues for stimulating and fruitful discussions on the topic of charge ordered multiferroics. In particular we would like to thank Marisa Medarde, Paolo Radaelli, Maxim Mostovoy, Serguei Brazovskii, Nicola Spaldin, Silvia Picozzi, Dimitry Efremov and Gianluca Giovannetti. We thank Serguei Brazovski for providing us with figure 7, Maxim Mostovoy for figure 9 and Silvia Picozzi for figure 12. The work of JvdB is supported by the Stichting voor Fundamenteel Onderzoek

der Materie (FOM). The work of DKh is supported by the Deutsche Forschungsgemeinschaft (DFG) via SFB 608.

References

[1] Fiebig M 2005 *J. Phys. D: Appl. Phys.* **38** 123
[2] Cheong S W and Mostovoy M 2007 *Nat. Mater.* **6** 13
[3] Hill N A 2000 *J. Phys. Chem.* B **104** 6694
[4] For a recent review, see, Khomskii D I 2006 *J. Magn. Magn. Mater.* **306** 1
[5] Katsura H, Nagaosa N and Balatsky A V 2005 *Phys. Rev. Lett.* **95** 057205
[6] Mostovoy M 2006 *Phys. Rev. Lett.* **96** 067601
[7] Efremov D V, van den Brink J and Khomskii D I 2004 *Nat. Mater.* **3** 853
[8] Efremov D V, van den Brink J and Khomskii D I 2005 *Physica* B **359** 1433
[9] van den Brink J and Khomskii D 1999 *Phys. Rev. Lett.* **82** 1016
[10] van den Brink J, Khaliullin G and Khomskii D 1999 *Phys. Rev. Lett.* **83** 5118
van den Brink J, Khaliullin G and Khomskii D 2001 *Phys. Rev. Lett.* **86** 5843
[11] For a review, see, van den Brink J, Khaliullin G and Khomskii D 2004 *Colossal Magnetoresistive Manganites* ed T Chatterji (Dordrecht: Kluwer)
[12] Efremov D V and Khomskii D I 2005 *Phys. Rev.* B **72** 012402
[13] Patterson C H 2005 *Phys. Rev.* B **72** 085125
[14] Ye F, Fernandez-Baca J A, Dai P, Lynn J W, Kawano-Furukawa H, Yoshizawa H, Tomioka Y and Tokura Y 2005 *Phys. Rev.* B **72** 212404
[15] Daoud-Aladine A, Rodriguez-Carvajal J, Pinsard-Gaudart L, Fernandez-Diaz M T and Revcolevschi A 2002 *Phys. Rev. Lett.* **89** 097205
[16] Wollan E O and Koeler W C 1955 *Phys. Rev.* **100** 545
[17] Goodenough J B 1955 *Phys. Rev.* **100** 564
[18] Grenier S, Hill J P, Gibbs D, Thomas K J, von Zimmermann M, Nelson C S, Kiryukhin V, Tokura Y, Tomioka Y, Casa D, Gog T and Venkataraman C 2004 *Phys. Rev.* B **69** 134419
[19] Wu L, Klie R F, Zhu Y and Jooss Ch 2007 *Phys. Rev.* B **76** 174210
[20] Jardon C, Rivadulla F, Hueso L E, Fondado A, Lopez-Quintela M A, Rivas J, Zysler R, Causa M T and Sanchez R D 1999 *J. Magn. Magn. Mater.* **196** 475
[21] Mercone S, Wahl A, Pautrat A, Pollet M and Simon C 2004 *Phys. Rev.* B **69** 174433
[22] Jooss Ch, Wu L, Beetz T, Klie R F, Beleggia M, Schofield M A, Schramm S, Hoffmann J and Zhu Y 2007 *Proc. Natl Acad. Sci.* **104** 13597
[23] Lopes A M L, Araújo J P, Amaral V S, Correia J G, Tomioka Y and Tokura Y 2008 *Phys. Rev. Lett.* **100** 155702
[24] Sanchez-Andujar M *et al* 2008 at press
[25] Mattis D C 1981 *Theory of Magnetism* (Berlin: Springer)
[26] Verwey E 1939 *Nature* **144** 327
[27] Verwey E J W and Haayman P W 1941 *Physica* **8** 979
[28] Alonso J A, Garca-Muñoz J L, Fernandez-Diaz M T, Aranda M A G, Martinez-Lope M J and Casais M T 1999 *Phys. Rev. Lett.* **82** 3871
[29] Mizokawa T, Khomskii D I and Sawatzky G A 2000 *Phys. Rev.* B **61** 11263
[30] Brazovskii S 2008 *Physics of Organic Superconductors and Conductors* (*Springer Series in Materials Sciences*) ed A G Lebed (Berlin: Springer)
[31] Special issue (whole) 1980 The Verwey transition *Phil. Mag.* **42** 835
[32] Anderson P W 1956 *Phys. Rev.* **102** 1008
[33] Rado G T and Ferrari J M 1975 *Phys. Rev.* B **12** 5166
[34] Rado G T and Ferrari J M 1977 *Phys. Rev.* B **15** 290
[35] Miyamoto Y and Chikazumi S 1988 *J. Phys. Soc. Japan* **57** 2040
[36] Miyamoto Y and Shindo M 1993 *J. Phys. Soc. Japan* **62** 1423
[37] Miyamoto Y, Ishihara S, Hirano T, Takada M and Suzuki N 1994 *Solid State Commun.* **89** 51
[38] Pauling L 1933 *J. Am. Chem. Soc.* **57** 2680
Pauling L 1938 *The Nature of the Chemical Bond* (Ithaca, NY: Cornell University Press)
[39] Bernal J D and Fowler R H 1933 *J. Chem. Phys.* **1** 515
[40] Castelnovo C, Moessner R and Sondhi S L 2008 *Nature* **451** 42
[41] Wright J P, Attfield J P and Radealli P G 2001 *Phys. Rev. Lett.* **87** 266401
Wright J P, Attfield J P and Radealli P G 2002 *Phys. Rev.* B **66** 214422
[42] Medrano C, Schlenker M, Baruchel J, Espeso J and Miyamoto Y 1999 *Phys. Rev.* B **59** 1185
[43] Khomskii D I 2007 *APS March Mtg* (Abstract A13.00006)
[44] Ikeda N, Kohn K, Myouga N, Takahashi E, Kitoh H and Takekawa S 2000 *J. Phys. Soc. Japan* **69** 1526
[45] Ikeda N, Ohsumi H, Ohwada K, Ishii K, Inami T, Kakurai K, Murakami Y, Yoshii K, Mori S, Horibe Y and Kitoh H 2005 *Nature* **436** 1136
[46] Nagano A, Naka M, Nasu J and Ishihara S 2007 *Phys. Rev. Lett.* **99** 217202
[47] Jona F and Shirane G 1962 *Ferroelectric Crystals* (Oxford: Pergamon)
[48] Monceau P, Nad F Y and Brazovskii S 2001 *Phys. Rev. Lett.* **86** 4080
[49] Kimura T, Goto T, Shintani H, Ishizaka K, Arima T and Tokura Y 2003 *Nature* **426** 55
[50] Lawes G, Kenzelmann M, Rogado N, Kim K H, Jorge G A, Cava R J, Aharony A, Entin-Wohlman O, Harris A B, Yildirim T, Huang Q Z, Park S, Broholm C and Ramirez A P 2004 *Phys. Rev. Lett.* **93** 247201
[51] Choi Y J, Yi H T, Lee S, Huang Q, Kiryukhin V and Cheong S-W 2008 *Phys. Rev. Lett.* **100** 047601
[52] Taniguchi K, Abe N, Takenobu T, Iwasa Y and Arima T 2006 *Phys. Rev. Lett.* **97** 097203
[53] Heyer O, Hollmann N, Klassen I, Jodlauk S, Bohaty L, Becker P, Mydosh J A, Lorenz T and Khomskii D 2006 *J. Phys.: Condens. Matter* **18** L471
[54] Arkenbout A H, Palstra T T M, Siegrist T and Kimura T 2006 *Phys. Rev.* B **74** 184431
[55] Jodlauk S, Becker P, Mydosh J A, Khomskii D I, Lorenz T, Streltsov S V, Hezel D C and Bohaty L 2007 *J. Phys.: Condens. Matter* **19** 432201
[56] García-Munoz J L, Rodrguez-Carvajal J and Lacorre P 1994 *Phys. Rev.* B **50** 978
[57] Sergienko I A and Dagotto E 2006 *Phys. Rev.* B **73** 094434
[58] Picozzi S, Yamauchi K, Sanyal B, Sergienko I A and Dagotto E 2007 *Phys. Rev. Lett.* **99** 227201
[59] Muñoz A, Alonso J A, Martinez-Lope M J, Casais M T, Martinez J L and Fernandez-Diaz M T 2001 *Inorg. Chem.* **40** 1020
[60] Sergienko I A, Sen C and Dagotto E 2006 *Phys. Rev. Lett.* **97** 227204
[61] Tokunaga Y, Lottermoser T, Lee Y, Kumai R, Uchida M, Arima T and Tokura Y 2006 *Nat. Mater.* **5** 937
[62] Hur N, Park S, Sharma P A, Ahn J S, Guba S and Cheong S-W 2004 *Nature* **429** 392
[63] Betouras J J, Giovannetti G and van den Brink J 2007 *Phys. Rev. Lett.* **98** 257601
[64] Harris A B 2007 *Phys. Rev.* B **76** 054447
[65] Kagomiya I, Matsumoto S, Kohn K, Fukuda Y, Shoubu T, Kimura H, Noda Y and Ikeda N 2003 *Ferroelectrics* **286** 167
[66] Chapon L C, Blake G R, Gutmann M J, Park S, Hur N, Radaelli P G and Cheong S-W 2004 *Phys. Rev. Lett.* **93** 177402

[67] Alonso J A, Casais M T, Martinez-Lope M J, Martinez J L and Fernandez-Diaz M T 1997 *J. Phys.: Condens. Matter* **9** 8515
[68] Blake G R, Chapon L C, Radaelli P G, Park S, Hur N, Cheong S-W and Rodriguez-Carvajal J 2005 *Phys. Rev.* B **71** 214402
[69] Kimura H, Kobayashi S, Fukuda Y, Osawa T, Kamada Y, Noda Y, Kagomiya I and Kohn K 2007 *J. Phys. Soc. Japan* **76** 074102
[70] Wang C, Guo G-C and He L 2007 *Phys. Rev. Lett.* **99** 177202
[71] Wang C and Guo G-C 2007 *Preprint* 0711.2539v1 [cond-mat.mtrl-sci]
[72] Giovannetti G and van den Brink J 2007 *Preprint* 0802.0653v1 [cond-mat.mtrl-sci]
[73] Ferrari V, Towler M and Littlewood P B 2003 *Phys. Rev. Lett.* **91** 227202